Table II
Comparison of Experimental Second-Order Rate Constants with Theoretical Limits for Termination Rate Constant[a]

approx. particle size, nm	second-order rate const[b]	theoretical termination rate const: lower limit[c] MMA[d]	lower limit[c] copolymer[e]	upper limit[c] MMA[d]	upper limit[c] copolymer[e]
500	5	9	14	145	270
50	50	3	45	41	780

[a] All rate constants expressed in L mol^{-1} s^{-1} at a temperature of 50 °C. [b] Radical disappearance rate constants experimentally measured for the acrylate copolymer as described in the text, for both 500-nm and 50-nm latices. Average conversion levels at the time of sampling were about 95% for the 500-nm latices and about 97% for the 50-nm latices. [c] Upper and lower limits calculated from the equations of Russell et al.[3] using 95% conversion for the 500-nm latex and 97% for the 50-nm latex. [d] Calculated from data of Ballard et al.[2] for a batch emulsion polymerization of pure MMA using k_p = 22 at 95% conversion and k_p = 12 at 97% conversion. (We have estimated their final particle size as roughly 160 nm.) [e] Calculated for the acrylate copolymer (see text) using k_p values of 170 for the 50-nm latex and 35 for the 500-nm latex (values taken from Lau et al.[1])

on the residual termination model. Russell et al. derived expressions for an upper limit and a lower limit for the termination rate constants in high-conversion free-radical polymerization systems. We have used their equations to calculate values for upper and lower limits for k_t for a polymerization of pure MMA at 50 °C and for our acrylate copolymer system at 50 °C to compare with the experimental data for our copolymer at that temperature; Table II summarizes the results. We have tried to make our comparisons with their theory at equivalent conversion levels, but the conversion at the time we begin the temperature treatment may be somewhat higher than the value at the time of sampling; thus, we regard our numbers and the comparison as approximate.

For both the large and small particle size systems, the experimental second-order rate constants fall near the lower limit predicted by the residual termination theory using our parameters. This trend is consistent with the behavior found by Russell et al.[3] at higher conversion levels. Since the experimental values are similar to those predicted by the theory, we think that the experimental second-order radical disappearance rate constants could provide a reasonable estimate for the termination rate constant during the polymerization. The interesting observation of faster termination in a 50-nm particle size latex having an average of half a radical per particle compared to that of the 500-nm particle size latex with up to 2000 radicals per particle suggests the termination step might be diffusionally controlled with chain transfer possibly involved. The postulated inhomogeneity of radical environments in the 500-nm particle size latices could also be a factor in the observed difference in termination rate. We plan further study of the termination mechanism and this difference.

Assuming our termination rate constants from the ESR study are a reasonable estimate of the termination rate of propagating radicals during the polymerization, this report to our knowledge represents the first direct experimental measurement of radical termination rate constants for an emulsion polymerization system. We can combine the termination rate constant data with our earlier results[1] to gain a more complete understanding of the kinetics of this system.[4] In future experiments, we plan to examine the propagating radicals without freezing the samples for a more direct analysis of the emulsion polymerization kinetics.

Acknowledgment. We thank Rohm and Haas Co. for supporting this research and permitting its publication. We are grateful to Professor D. H. Napper for helpful discussions and for sharing results prior to publication.

Registry No. BA, 141-32-2; MMA, 80-62-6; MAA, 79-41-4.

References and Notes

(1) Lau, W.; Westmoreland, D. G.; Novak, R. W. *Macromolecules* **1987**, *20*, 457.
(2) Ballard, M. J.; Gilbert, R. G.; Napper, D. H.; Pomery, P. J.; O'Sullivan, P. W.; O'Donnell, J. H. *Macromolecules* **1986**, *19*, 1303.
(3) Russell, G. T.; Napper, D. H.; Gilbert, R. G. *Macromolecules* **1988**, *21*, 2133.
(4) Direct elucidation of major kinetic parameters (k_p, k_t, initiator efficiency, and activation energy) will be discussed more fully in a separate report.

David G. Westmoreland and Willie Lau*
Research Laboratories, Rohm and Haas Company
Spring House, Pennsylvania 19477

Received August 30, 1988;
Revised Manuscript Received November 2, 1988

Studies of Liquid Crystalline Polymer Phase Transitions Using Synchrotron X-Radiation

Little more than a decade ago liquid crystallinity in polymers was first recognized. Since that time the numbers and types of newly synthesized liquid crystalline polymers (LCPs) have increased rapidly. A number of entirely aromatic LCPs, which are thus stiff and insoluble, have recently been commercialized. In addition to the commercial polymers, many polymers containing both mesogenic units and flexible spacers have been the subject of extensive study around the world. The mesogenic units and flexible spacers either may appear in the main polymer chain or the mesogenic units may be attached by spacers to a polymer backbone in the so-called side-chain LCPs. The use of flexible spacers has also resulted in the lowering of melting points in LCPs, and more recently substituents have been added to the mesogenic groups thereby inducing solubility in common organic solvents while maintaining the LC properties.[1,2]

We have become interested in the physical nature of the mesophase and in studying the mesophase transitions of model LCPs. In this paper we describe recent studies of LCP mesophases and mesophase transitions studied by using real-time X-ray diffraction experiments made possible by the use of synchrotron radiation. Specifically, variations in X-ray diffracted intensities were used to follow transitions from the LCP mesophase to the isotropic melt. We were interested in studying not only the rate of transition but also the biphasic behavior of selected liquid crystalline polymers.

The mesogenic structures of the LCPs investigated in this study are shown below:

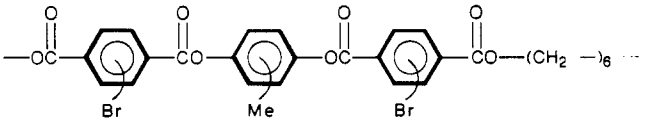

BP6

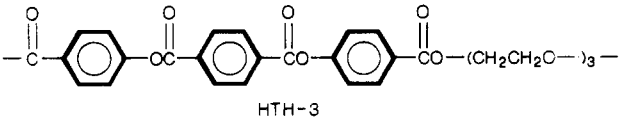

HTH-3

The BP6 polymer with a spacer composed of 6 methylene units is unusual in that it has an irregular mesogenic

0024-9297/89/2222-0498$01.50/0

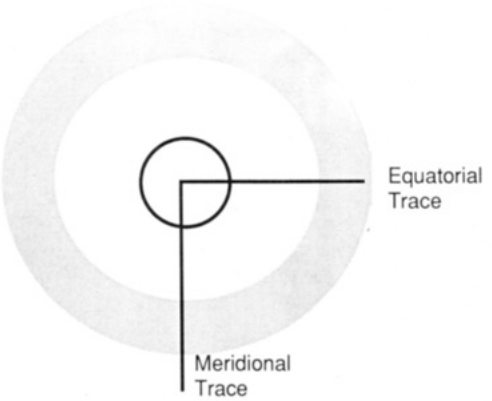

Figure 1. Schematic of recorded X-ray spectra of the LC polymer sample.

structure which imparts solubility in common organic solvents (THF, $CHCl_3$, CH_2Cl_2). BP6 lacks any transition that can be associated with melting. The HTH-3 polymer with a spacer of three ethylene oxide units has good solubility in CH_2Cl_2 but is a semicrystalline polymer in that it possesses a distinct melting transition. The synthesis of the polymers used in this study and some of their physical characteristics have been reported elsewhere.[1,3] Fibers of the BP6 polymers were formed by taking molten polymer heated on a Fisher-Johns melting point apparatus and drawing out the melt with tweezers.

X-ray diffraction data were obtained at the Cornell High Energy Synchrotron Source (CHESS) facilities at Cornell University. The polymer samples, oriented fibers, and powders were examined by using a Mettler hotstage mounted in the beam path to control sample temperatures. Temperatures and heating rates for the experiments ranged from 50 to 270 °C and 10 to 20 deg/min, respectively. Mylar films or glass cover slips were used to hold the samples in place in the hotstage. The A1 beamline used at CHESS produces monochromated X-radiation with a 0.154-nm wavelength. The diffracted intensity was collected with an image intensifier which enhanced the X-ray diffracted intensity incident on a fluorescent screen. The images were then photographed with a video camera for both simultaneous storage on digital videotape and transmission to a television monitor. The diffractograms stored on digital videotape were analyzed and enhanced with an RCI Framestore image processor. Data were recalled from videotape as intensity versus pixel position where the pixel position corresponded to x–y coordinates on a conventional flat film diffraction pattern. The methods of extracting the resulting data were used as shown schematically in Figure 1. Radial traces through the center of the diffractogram were plotted as intensity versus pixel number. Background was removed by use of a baseline subtraction routine.

The BP6 polymer is a liquid crystal glass and possesses no crystallinity as evidenced by X-ray diffraction studies of these polymers at room temperature, a temperature below the T_g for this polymer. The values of the softening temperature of 127 °C and the isotropic clearing temperature, T_i, of 290 °C were obtained by visual observation using a polarizing optical microscopy. Differential scanning calorimetry (DSC) traces did not exhibit any thermal transitions other than the glass transition.[1] Any melting or clearing endotherms, if present, must therefore be exceedingly small or broad.

Figure 2 shows the recorded diffraction pattern that was obtained from an oriented BP6 fiber at room temperature by using a flat film camera and a conventional source. Two

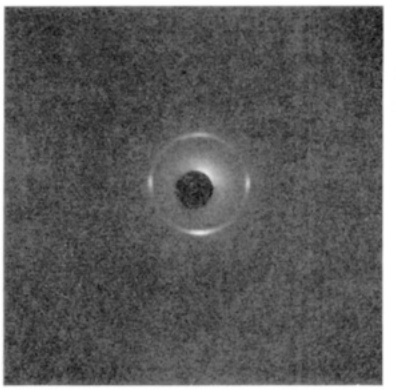

Figure 2. WAXD spectrum of oriented BP6.

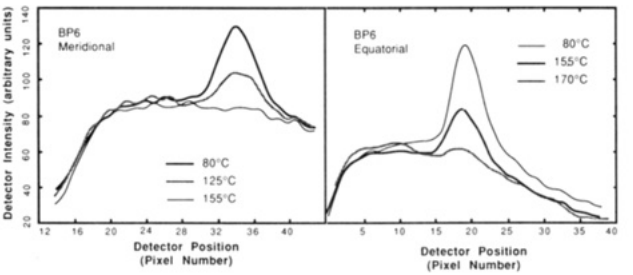

Figure 3. Plots of (a, left) meridional and (b, right) equatorial intensities versus pixel number for BP6.

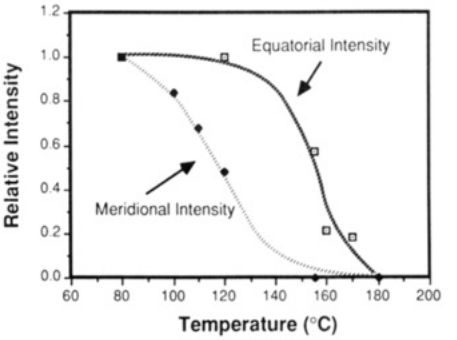

Figure 4. Plot of relative intensity versus temperature for individual equatorial and meridional arc intensities of BP6.

surprising features were observed in these diffractograms. First, there are two sets of arcs perpendicular to each other, both sets corresponding to a d-spacing of 1.26 nm. Second, one set of arcs was observed to disappear at a lower temperature than the other set in the dynamic X-ray experiments. DSC revealed no type of transition that could be correlated with the rapid decrease in intensity of either set of arcs.

The intensity of the meridional peak shown in Figure 3a started to decrease as soon as 120 °C was reached. This temperature, 120 °C, is associated with the onset of biphasic behavior seen in the optical microscope as well as softening of the polymer. By contrast, in the equatorial scans of BP6 shown in Figure 3b, the peak at pixel position 20 (1.26 nm) was observed to decrease with increasing temperature above 150 °C, while the rest of the diffractogram remained unchanged. The integrated diffracted intensity under the radial traces of both the meridional and equatorial arcs are plotted separately as a function of temperature in Figure 4. If the two curves in Figure 4 are considered collectively, it becomes less surprising that no transition was observed by DSC. The isotropic transition is simply too broad to produce a discernible peak. Optical micrographs substantiate that an isotropic mesophase coexists with the smectic mesophase over a broad temperature range. The d-spacing of 1.26 nm is smaller than

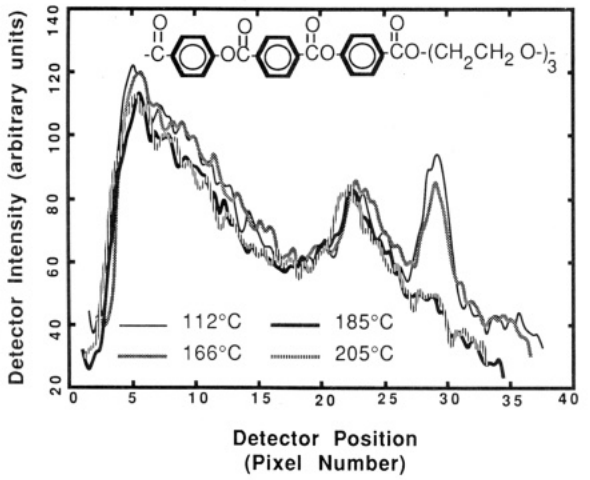

Figure 5. Recorded WAXD spectra of HTH-3 at (a) 112, (b) 166, (c) 185, and (d) 205 °C.

the extended monomeric repeat distance and may be indicative of a smectic C mesophase.

In contrast to the behavior of BP6, polymer HTH-3 is a semicrystalline polymer that exhibits both a very sharp melting transition and a pronounced clearing transition by DSC.[3] Also previously noted is an intermediate transition associated with a smectic–nematic phase transition. All transitions have been readily observed by optical microscopy. Describing the results of the dynamic X-ray studies of HTH-3 powder, Figure 5 shows the recorded intensity versus pixel position taken at four temperatures. The temperature range of observation was from the crystalline solid and the lower temperature smectic mesophase. As shown in the figure, the peak at pixel number 30 (0.45 nm) disappeared between 166 and 185 °C. Over this temperature range the melting transition took place and with this polymer we can therefore correlate DSC and dynamic X-ray behavior. Note that the peak at pixel number 7 (2.5 nm) did not change nor did the peak at pixel number 23. The latter peak is associated with the Mylar sample holder. The inner ring is associated with the smectic mesophase of HTH-3 and is qualitatively different than the inner ring of BP6. HTH-3 has previously been assigned a higher order smectic phase whereas we believe that BP6 has a smectic C mesophase.

The use of synchrotron radiation to study LCPs enables several types of experiments not previously possible. Not only may the phase transitions and biphasic behavior be observed in real time as the temperature is changes as discussed in the present paper, but the diffractograms can be recorded on a time scale which makes determination of the transition rates possible. We are presently studying the phase transitions in these and other LCPs and will report the results of such investigations in due course.

Acknowledgment. We thank the Cornell Materials Science Center (MSC) funded through NSF for financial support, use of the MSC facilities, and a fellowship for A.D. Financial assistance from the AT&T Foundation is greatly appreciated. We also thank the Cornell High Energy Synchrotron Source (CHESS) funded through NSF DMR 84-12465 for use of the facility. Finally, we thank Scott McNamee, Don Buckley, and Professors Ed Kramer and David Grubb for help with the CHESS run.

Registry No. BP6, 117939-37-4; HTH-3, 84329-77-1.

References and Notes

(1) Delvin, A.; Ober, C. K. *Polym. Bull.* **1988**, *20*, 245.
(2) Delvin, A.; Ober, C. K.; Bluhm, T. L. *Polym. Mater. Sci. Eng.* **1988**, *58*, 1029.
(3) Galli, G.; Chiellini, E.; Ober, C. K.; Lenz, R. W. *Makromol. Chem.* **1982**, *183*, 2693.

A. Delvin and C. K. Ober*
Materials Science & Engineering
Cornell University, Ithaca, New York 14853

T. L. Bluhm
Xerox Research Centre of Canada, 2660 Speakman Dr.
Mississauga, ON L5K 2L1 Canada

Received August 23, 1988

Fourier Transform Raman Studies of Secondary Structure in Synthetic Polypeptides

The importance of α-helical and the β-sheet structures on the function of both fibrous and globular proteins is well established. What is less well-known is the interrelated role of primary and secondary structures and how that influences the tertiary structure responsible for protein function. Energy calculations do not yet have the sophistication to resolve this puzzle, but some progress is being made at the experimental forefront particularly with the advent of a new technique known as Fourier transform Raman spectroscopy (FT Raman) which is described herein.

In the structural characterization of biomolecules, Raman spectroscopy has always been the technique of choice due to the problems associated with obtaining an infrared (IR) spectrum in native (usually aqueous) environments.[1] In addition, Raman spectroscopy is a noninvasive technique since usually no change in the sample or its environment occurs during structural characterization. Thus, molecules in solution pose no more of a problem than an opaque solid, and in both cases after a Raman investigation, neither the initial molecular structure nor the morphology has been altered.

On the less positive side, a Raman spectrum of a biopolymer or a protein is often unobtainable using visible excitation due to the presence of a fluorescent impurity.[2] Absorption by this impurity leads to electronic transitions followed by emission which is not spontaneous but occurs over a time interval through a manifold of intermediate states. This fluorescent emission is so efficient (high quantum yield) that its intensity will completely or, at best, partially obscure the Raman spectrum of the biomolecule of interest. In cases where the impurity chromophore does not fluoresce, it may cause local heating due to photon absorption which could subsequently lead to degradation or denaturation if the biomolecule is a protein.

Recently Raman spectroscopy has entered the Fourier domain using cw Nd:YAG excitation in the near IR at 1.064 μm.[3,4] Although photons with such a low energy cannot excite fluorescence, they still give rise to Raman scattering as indicated in Figure 1a. As shown, the frequency regime of the Stokes-shifted Raman scattering using a Nd:YAG laser is considerably lower than that using argon ion excitation. In fact, the Stokes FT Raman spectrum occurs on the lower end of the frequency region, usually referred to as the near infrared. In this region, standard Fourier transform IR (FTIR) instruments have been routinely used to make IR transmission measurements for more than 20 years. It soon became obvious that the conventional Raman dispersion spectrometer which is used for spectral analysis in the visible should be replaced by the higher throughput, multiplex FTIR instrument for analysis of Raman scattering in the near infrared. The result is schematically illustrated in Figure 1b. As

0024-9297/89/2222-0500$01.50/0